MARK/PAR1 kinase is a regulator of microtubule-dependent transport in axons

Eva-Maria Mandelkow, Edda Thies, Bernhard Trinczek, Jacek Biernat, and Eckard Mandelkow

Max-Planck Unit for Structural Molecular Biology, 22607 Hamburg, Germany

Microtubule-dependent transport of vesicles and organelles appears saltatory because particles switch between periods of rest, random Brownian motion, and active transport. The transport can be regulated through motor proteins, cargo adaptors, or microtubule tracks. We report here a mechanism whereby microtubule associated proteins (MAPs) represent obstacles to motors which can be regulated by microtubule affinity regulating kinase (MARK)/Par-1, a family of kinases that is known for its involvement in establishing cell polarity and in phosphorylating tau protein during Alzheimer neurodegeneration. Expression of MARK causes the phosphorylation of MAPs at their KXGS motifs, thereby detaching MAPs from the microtubules and thus facilitating the transport of particles. This occurs without impairing the intrinsic activity of motors because the velocity during active movement remains unchanged. In primary retinal ganglion cells, transfection with tau leads to the inhibition of axonal transport of mitochondria, APP vesicles, and other cell components which leads to starvation of axons and vulnerability against stress. This transport inhibition can be rescued by phosphorylating tau with MARK.

Introduction

Microtubule-dependent transport by motor proteins is a major mechanism for distributing vesicles or organelles in the cell. Examples are endocytosis or exocytosis of vesicles, the distribution of mitochondria or peroxisomes, or the separation of chromosomes during mitosis (Terada and Hirokawa, 2000; Kamal and Goldstein, 2002). Active transport is particularly important when cells become asymmetric (e.g., the axons of neuronal cells) or when cell components have to be transported against a concentration gradient (e.g., the RNA-containing P-granules in zygotes). The tracks are provided by the polar microtubule network, the motion is generated by motor proteins with built-in directionality (kinesin usually toward the cell periphery, "outbound", dynein toward the cell interior, "inbound"), and cargoes are attached by adaptor complexes. Given the crowded interior of a cell, this poses the problem of how the delivery of cargoes is regulated. Linkage to the right adaptors and motors is a key decision, but even if that is achieved, movement in the right direction is not ensured unless an open path is provided. Here, we are concerned with traffic control by phosphorylation which has been suspected to contribute to the regulation. For example, motor proteins can be phosphorylated and kinases influence vesicle attachment (Lee and Hollenbeck, 1995; Lopez and Sheetz, 1995; Sato-Harada et al., 1996; Morfini et al., 2002), but the connection between kinases, target proteins, and motility has remained elusive.

Microtubule tracks are covered with microtubule associated proteins (MAPs), which contribute to their stabilization that is important for cell shape or neurite outgrowth (Drubin and Kirschner, 1986; Kosik and McConlogue, 1994; Cassimeris and Spittle, 2001; Baas, 2002; Biernat et al., 2002). In addition MAPs can compete with motors for microtubule binding (Lopez and Sheetz, 1993; Hagiwara et al., 1994). Our earlier experiments with CHO cells transfected with tau protein revealed an inhibition of transport, with the consequence that organelles clustered in the cell interior (Ebneth et al., 1998). Analysis of organelle flux showed that both types of microtubule motors (kinesin and dynein) become inhibited by tau, but kinesin is more affected so that dynein dominates. Furthermore, experiments with single molecules showed that elevated concentrations of tau on the microtubule surface leads to a reduced attachment of kinesin (Seitz et al., 2002). Analysis of the transport inhibition by tau in neurons showed that the flux of mitochondria and vesicles containing amyloid precursor protein (APP) down the axon is disturbed, resulting in the degeneration of the axons (Stamer et al., 2002). The results suggested a new relationship between tau and APP, the two proteins which play a key role in Alzheimer's disease.

The online version of this article contains supplemental material.

Correspondence to Eva Marie Mandelkow: mandelkow@mpasmb.desy.de

B. Trinczek's present address is Dept. of Medicinal Chemistry, University of Kansas, Lawrence, KS 66045.

Abbreviations used in this paper: APP, amyloid precursor protein; MAP, microtubule associated protein; MARK, microtubule affinity regulating kinase; RGC, retinal ganglion cell.

The Journal of Cell Biology, Vol. 167, No. 1, October 11, 2004 99–110
http://www.jcb.org/cgi/doi/10.1083/jcb.200401085

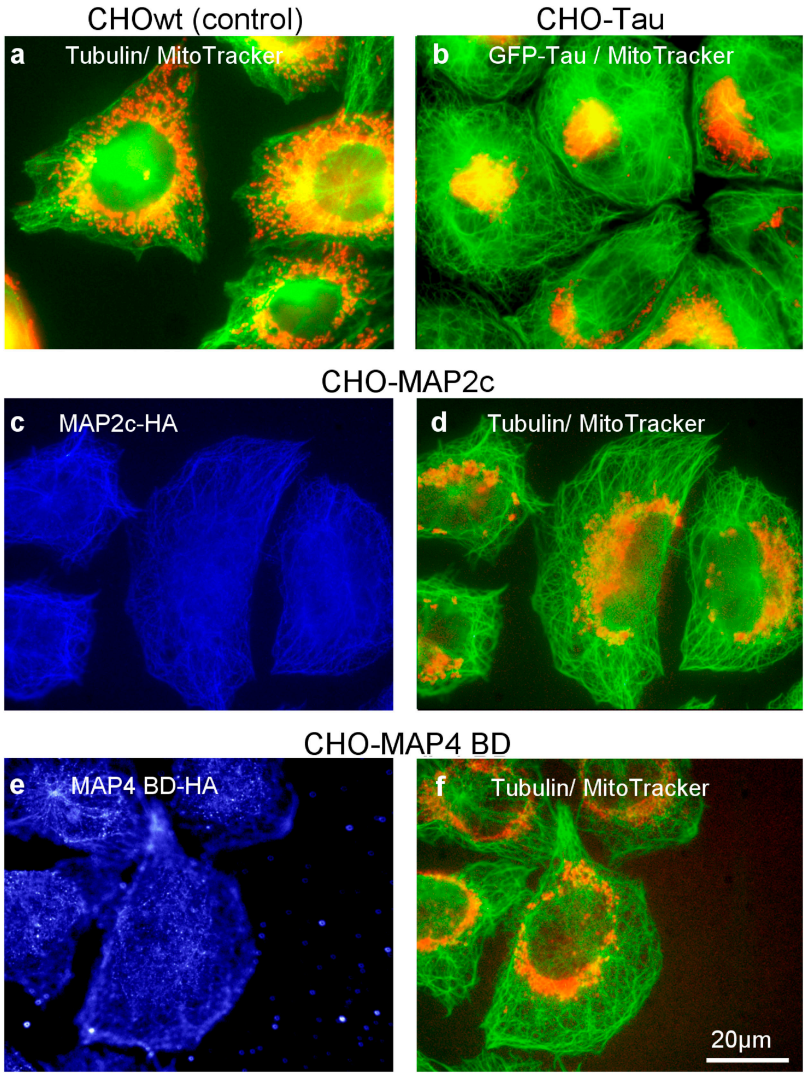

Figure 1. **Inhibition of plus-end directed transport of mitochondria by tau, MAP2c, and MAP4.** (a) Untransfected CHO control cells stained for tubulin (green) and mitochondria (MitoTracker, red). Note that mitochondria are distributed throughout the cell. (b) CHO cell stably transfected with GFP-tau. (c) CHO cells stably transfected with MAP2c (HA-tagged, blue), (d) stained for tubulin (green) and mitochondria (red, yellow). (e) CHO cells stably transfected with MAP4-BD (HA tagged), (f) stained for tubulin and mitochondria. Note that all MAPs in b–e cause clustering of mitochondria at the MTOC.

The kinases and phosphorylation sites of MAPs have been studied extensively in the context of microtubule stabilization and neurodegeneration, especially for the case of tau protein (Garcia and Cleveland, 2001; Lee et al., 2001). Certain kinases are particularly efficient in detaching MAPs from microtubules; the best examples are the microtubule affinity regulating kinase (MARK)/Par1 kinases, which phosphorylate the KXGS motifs in the repeat domains of MAP4, MAP2, or tau (Drewes et al., 1997). Increasing the activation of MARK by expression of MARK or its activating kinase MARKK leads to microtubule breakdown and cell death (Ebneth et al., 1999; Timm et al., 2003). Homologous kinases (PAR-1) play a role in cell polarity development (Kemphues, 2000; Riechmann and Ephrussi, 2001; Cohen et al., 2004) or in neurite outgrowth (Biernat et al., 2002). To study the influence of MAP phosphorylation on vesicle and organelle transport we used different cell models. We generated CHO cells inducibly expressing MARK2, labeled vesicles and organelles with fluorescent markers, and traced them by live cell microscopy. To study the influence of tau phosphorylation on axonal transport in primary retinal ganglion neurons we transfected them with YFP-MARK2 and CFP-tau by adenoviruses. Here, we show that different MAPs have similar inhibitory effects on microtubule-based transport which are relieved by kinases of the MARK family that reduce the level of microtubule-bound MAPs and thus remove obstacles from the microtubule surface. In retinal ganglion cells (RGCs) we demonstrate that the inhibition of axonal transport by tau is rescued by the activity of MARK2, which phosphorylates tau at the KXGS motifs and, thus, detaches it from the microtubule tracks. This has implications for the neurodegeneration in Alzheimer's disease where the phosphorylation of tau by kinases of the MARK family is enhanced.

Results

Transport inhibition by MAPs

MAPs are known as stabilizers of microtubules and promoters of neurite outgrowth. In the case of the neuronal tau protein another potential function is the regulation of intracellular traffic (Ebneth et al., 1998). This ability of tau appears to be rather general, it occurs in all cell types where tau is expressed, and it affects all cargoes transported along microtubules tested so far (vesicles, organelles, intermediate fila-

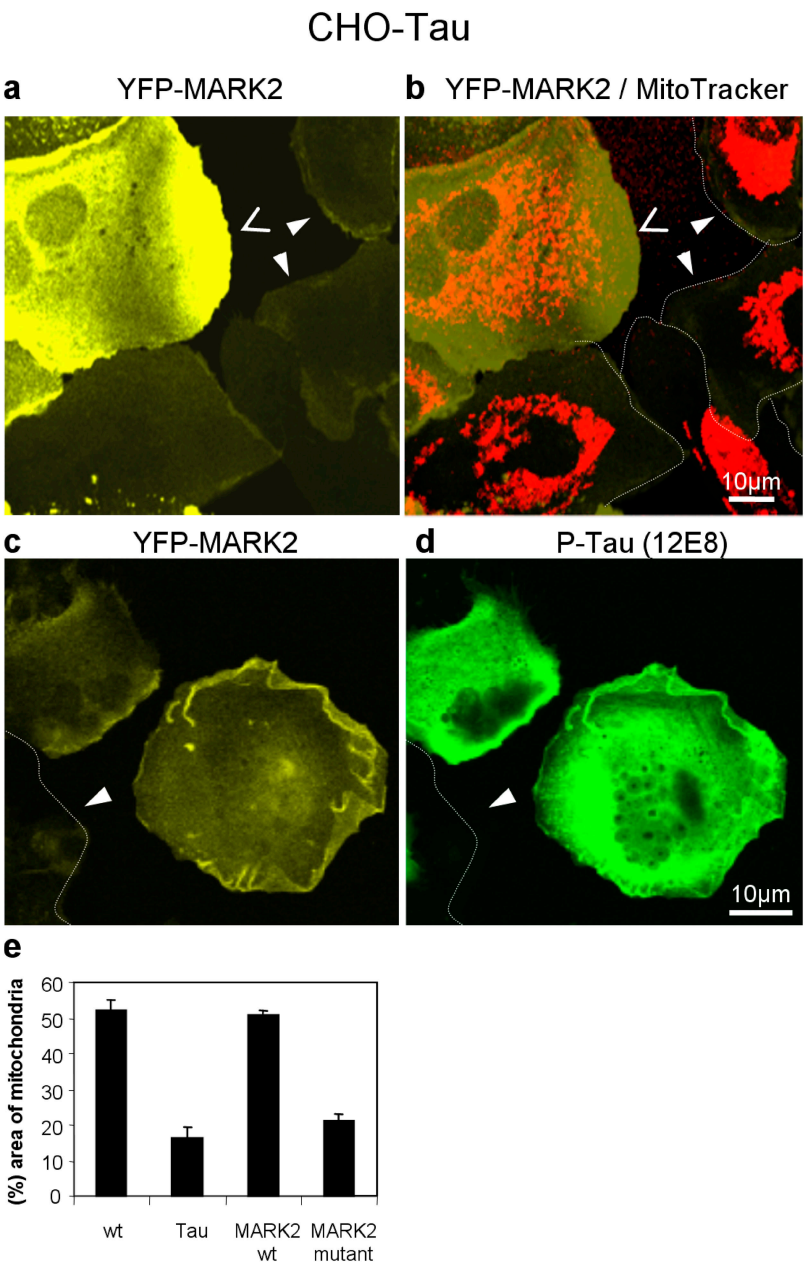

Figure 2. **Recovery of plus-end transport of mitochondria by coexpression of tau and MARK2.** (a and b) CHO cells stably expressing tau and cotransfected with YFP-MARK2 (a, yellow and open arrowhead). In cells not expressing MARK2, mitochondria are clustered around the MTOC (closed arrowheads, cell perimeters dotted white), whereas the cell expressing MARK2 (top left) shows redispersion because the block of transport is partially relieved. (c and d) Correlation between MARK2 expression and tau phosphorylation at KXGS motifs (12E8 antibody). (c) Distribution of YFP-MARK2 (yellow) and (d) the same cells contain tau with elevated phosphorylation (green). Arrows point to untransfected cell not showing phosphorylation of MARK2 and tau. (e) Comparison of distribution of mitochondria. In wild-type CHO cells ~50% of the cytoplasm is populated by mitochondria. The fraction is reduced to ~15% after transfection with tau, but nearly restored after additional transfection with MARK2. The inactive MARK2 mutant cannot rescue the clustering caused by tau.

ments, etc.). Because tau is a neuronal MAP it was of particular interest for neurodegeneration in Alzheimer's disease where traffic along microtubules is interrupted (Stamer et al., 2002). However, it was an open question whether other MAPs in other cell types could affect microtubule transport in a similar fashion. We addressed this issue by studying MAP2 and MAP4, two major types of MAPs. CHO cells were stably transfected with MAP2c (the juvenile short isoform of the neuronal MAP2) or MAP4-BD, the microtubule-binding domain of the ubiquitous MAP4 (Olson et al., 1995), and the transport of vesicles, mitochondria, peroxisomes, or vimentin intermediate filaments was monitored (Fig. 1). In each case one observes an inhibition of net outward transport which results in the clustering of the cargoes in the cell center. In wild-type cells, mitochondria are distributed throughout the cytoplasm (Fig. 1 a), but in stably MAP-transfected cells they congregate around the MTOC (Fig. 1, b, d, and f). This effect is reminiscent of that of tau and is explained by a general inhibition of motor proteins which affects kinesin more than dynein so that the centripetal movements dominate (Trinczek et al., 1999). The effect depends on the affinity and concentration of MAPs, i.e., low levels of MAPs or loosely bound MAP constructs have only little effect on traffic. Because the binding of MAPs to microtubules is regulated by phosphorylation one would expect that kinases that detach MAPs from microtubules would relieve the inhibition of motors. One kinase family that detaches tau, MAP2, and MAP4 efficiently from microtubules is MARK, which phosphorylates the KXGS motifs in the repeat domain of these MAPs (Illenberger et al., 1996). Thus, a major aim of this work was to find out whether kinases of the MARK family could indeed counteract the transport inhibition by MAPs.

MARK relieves transport inhibition by MAPs

When trying to observe the detachment of MAPs experimentally one is faced with the dual consequences of phosphorylation by MARK: detachment of MAPs may clear the microtubule tracks and thus facilitate traffic, but bare microtubules are less stable and tend to disintegrate, thereby interrupting traffic altogether. In CHO cells (which have a low level of endogenous MAP4), transient transfection with MARK causes the rapid disintegration of microtubules (with subsequent cell death), and the level of phospho-MAP4 remains below detectability by immunofluorescence (Ebneth et al., 1999). If these cells are stably transfected with tau, MAP2c, or MAP4-BD in order to visualize the inhibition of traffic (e.g., by the clustering of mitochondria, as in Fig. 1, b, d, and f), microtubules are stabilized and cells remain viable. In this case the transfection of MARK suffices to make the phosphorylation of MAPs visible (Fig. 2, c and d; Ebneth et al., 1999). But it has been difficult to demonstrate how the phosphorylation of MAPs leads to the reversal of transport inhibition. The reason is that too much phosphorylation causes not only detachment of MAPs and clearance of the microtubule tracks, but also breakdown of microtubules, whereas too little phosphorylation does not rescue the transport inhibition. This means that one has to match the concentration of MAPs with the activity of MARK in a controlled fashion.

To achieve this we tested different transfection systems, including a MARK2-inducible cell line (tet-on), to control the expression and activity of the kinase. The best results were obtained with the adenovirus transfection protocol (He et al., 1998, Stamer et al., 2002). Because MARK2 was tagged with YFP and mitochondria with MitoTracker it was possible to monitor MARK2 and mitochondria simultaneously in living cells. In the tau-stable CHO cell line mitochondria are clustered near the MTOC (Fig. 2 b, closed arrowheads), but when the cells are transfected with MARK2 the mitochondria become dispersed again (Fig. 2 b, open arrowheads). The expression of MARK2 is accompanied by strong enhancement of tau phosphorylation at the KXGS motifs (Fig. 2, c and d, 12E8 antibody), consistent with tau's detachment from microtubules and the release of the traffic blockade. Thus, MARK and tau operate in an antagonistic fashion. Quantification shows that ~50% of the cytoplasm is occupied by mitochondria in control cells, which decreases to ~15% after tau transfection. The traffic blockade can be relieved by MARK2, but not by the kinase-dead MARK2 mutant (Fig. 2 e).

MARK facilitates endogenous traffic in cells

Our next aim was to monitor the movement of vesicles or organelles along microtubules and to record the parameters of speed, run length, changes in direction, and how they depend on kinases such as MARK. To test whether the phosphorylation of MAPs and their detachment from microtubules would lead to changes in mobility we expressed MARK2 in a controlled fashion in CHO cells under the inducible tet-on expression protocol (Gossen and Bujard, 2002) and chose early time points of

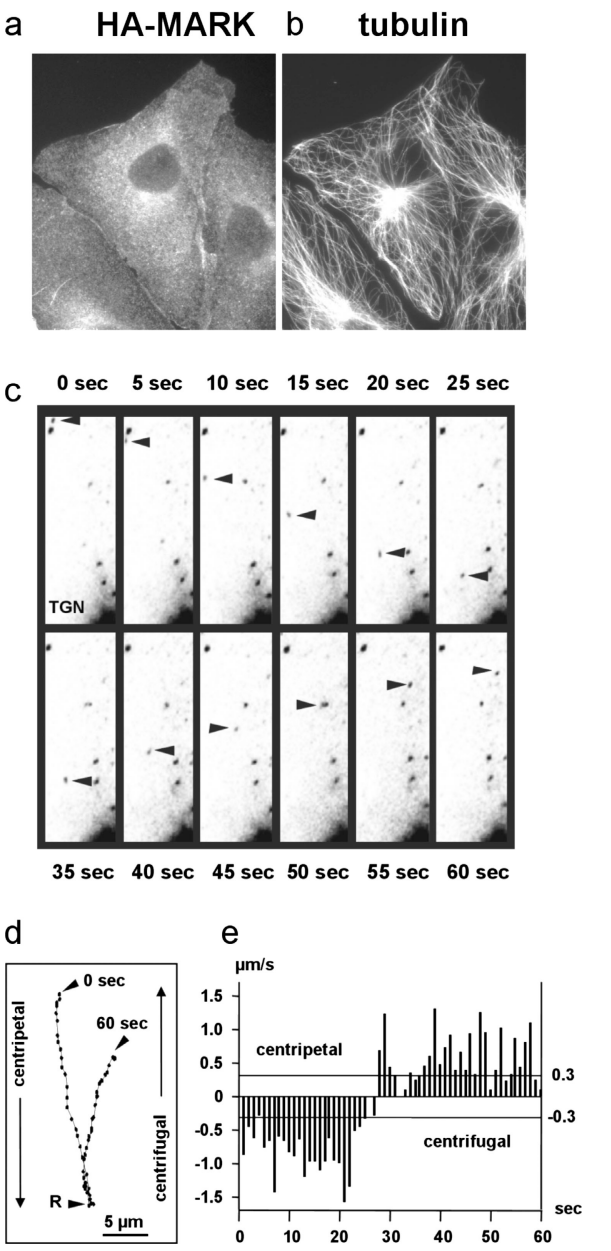

Figure 3. **Motion analysis of vesicles and organelles.** MARK2 is expressed inducibly in CHO cells under the control of the tetracycline responsive promoter. (a) Upon induction with 1 µg/ml doxycyclin for 12–18 h, HA-tagged MARK2 becomes detectable by the polyclonal rabbit HA-tag antibody in the cells (~100% in the induced state). Because prolonged periods of MARK expression (24–72 h) destroy the microtubule network the motility assays were done at earlier time points where >90% of cells have normal microtubules and the MTOC is preserved. (b) Immunofluorescence of cells by anti-tubulin antibody DM1A showing that most cells are HA-MARK positive (a) and have a normal microtubule network. (c) The movement of an individual vesicle (arrowheads) was recorded during a period of 60 s (shown in 5-s intervals). TGN identifies the trans-Golgi network that was taken as a reference to distinguish between centripetal and centrifugal movements. (d) Single particle tracking of the vesicle shown in panel a during the 60 s with higher time resolution (1 s). The starting and end points are indicated by arrowheads. Note the reversal in direction at point R. (e) Instantaneous velocities of vesicle shown in panels c and d versus time. The diagram distinguishes between centripetal (toward the TGN, negative values) and centrifugal (away from the TGN, positive values) movements of the vesicle. Velocities below 0.3 µm/s (marked by horizontal lines) were counted as Brownian motion rather than motor-driven movement and not used in the subsequent statistical analysis.

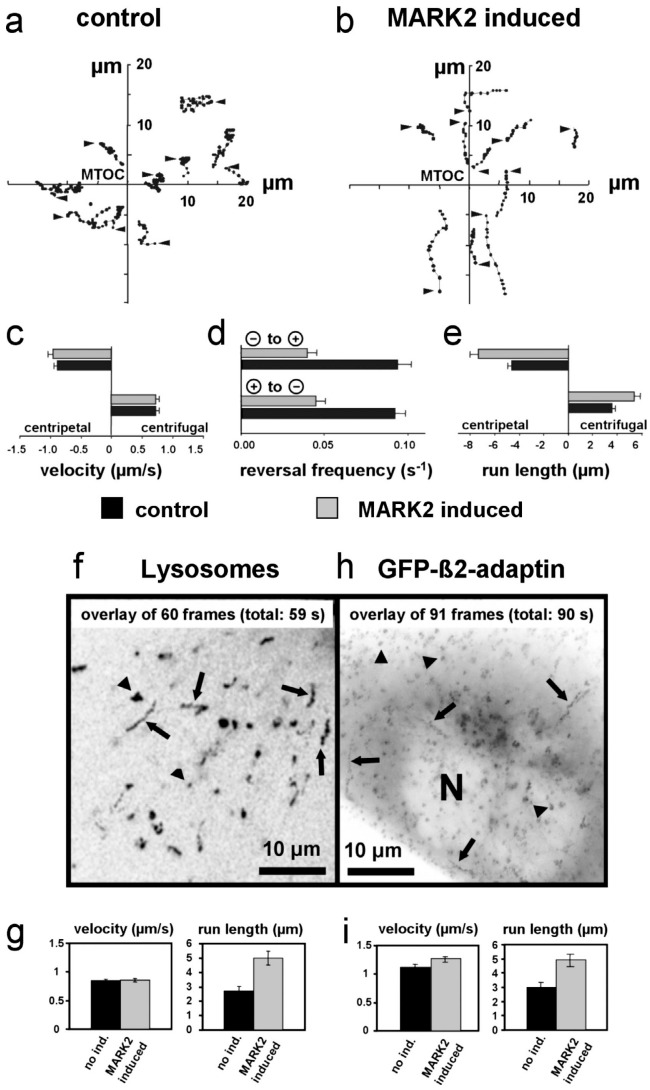

Figure 4. **Influence of MARK2 on the transport of vesicles and organelles.** (a) Tracking pattern of GFP-VSVG–tagged vesicles in noninduced CHO cells (controls) and (b) in MARK2-induced CHO cells. Dots connected by a line identify consecutive positions of a vesicle (1-s time intervals, arrowheads indicate starting points). The coordinates are centered on the TGN (labeled strongly with GFP-VSVG) near the microtubule organizing center. Upon MARK induction the tracks become longer and straighter, indicating that fewer directional changes occur. (c–e) Quantification of GFP-VSVG–tagged vesicle movement in noninduced CHO cells (black bars) and MARK2-induced cells (gray bars). The data are based on the vesicle motion recorded from 30 cells, 150 vesicles were analyzed, error bars = SEM. (c) Velocities remain unchanged after the induction of MARK2 in either direction (inbound v$\sim$0.9µm/s, outbound $\sim$0.7 µm/s; $n > 500$). (d) Reversal frequencies decrease strongly after MARK2 induction ($\sim$0.04 s^{-1} with MARK2, $\sim$0.09 s^{-1} without MARK2, both for inbound/outbound and outbound/inbound reversals; $n > 100$). (e) Run lengths increase strongly ($\sim$50%) upon MARK2 induction in both directions ($n > 100$). Note that both with and without MARK2 the inbound run lengths are $\sim$30% longer than outbound (4.6 µm inbound, 3.6 µm outbound without MARK2). (f and g) Motion of lysosomes. (f) This panel shows an overlay of 60 images separated by 1 s. Lysosomes move on linear tracks >1 µm (arrows). Particles that are immobile or show only short Brownian movements ($\leq$0.3 µm and random direction) can also be observed (spots marked by arrowheads). (g) Velocities remain unchanged upon MARK2 induction ($\sim$0.8 µm/s), but run lengths increase (from 3 to 5 µm). Reversal frequencies and directionalities cannot be determined because in CHO cells labeled with LysoTracker there is no internal reference indicating the cell's interior. (h) Endocytotic vesicles: CHO cells were transiently transfected with EGFP-labeled β2-adaptin, a marker of the AP-2 complex of endocytotic clathrin-coated vesicles. During the time of observation shown here (90 s) fluorescent paths are clearly visible. Linear or curved tracks longer than 1 µm represent actively transported vesicles (arrows), broader black or gray spots represent immobile particles and/or vesicles showing Brownian motion (arrowheads). The overexpression of GFP/β2-adaptin causes a strong background noise in the cytoplasm and the nucleus (N) becomes visible. The rather immobile fluorescent patches in the more peripheral regions of the cell are clathrin-coated vesicles or their precursors (arrowheads; Laporte et al., 1999). In the interior of the cell near the nucleus (N) an accumulation of the fluorescent signal can be observed suggesting that EGFP/β2-adaptin also colocalizes with the exocytotic and/or endosomal compartment. This is supported by the occurrence of fast moving vesicles entering or leaving this area. In contrast to the post-Golgi vesicles labeled by transient transfection of GFP-VSVG, the system here cannot provide reversal frequencies because of the strong background that shortens the time in which the particles are clearly seen in focus. (i) Velocities remain unchanged by MARK2 ($\sim$1 µm/s), but run lengths increase almost twofold. The tracks illustrate three scenarios: the period of motion observed within the plane of focus is flanked by (1) periods of active transport out of focus, (2) resting states in focus and active transport out of focus, and (3) periods of pauses in focus. We only analyzed events of movement which were clearly in focus and which show at least two stop events in order to determine the run length. As in the case of lysosomes (g), the velocity of vesicles (i) remains roughly the same after MARK2 induction, but there is a notable increase in the run length. Error bars indicate SEM.

MARK2 expression where the microtubule network was still intact. Fig. 3 a shows the punctate distribution of MARK2. The microtubule network is still intact, and there is no sign of colocalization of MARK2 with microtubules (Fig. 3 b).

Exocytotic vesicles can be visualized by GFP-tagged VSV-G protein (Scales et al., 1997). Fig. 3 (c–e) shows an example of a particle moving initially to the cell center, then reversing to the periphery. In the motion analysis we record the direction, instantaneous velocity, run length, and the frequency of reversals (Trinczek et al., 1999). The outbound motion depends essentially on the plus-end motor kinesin, inbound motion on the minus-end motor dynein. Elevation of MAPs such as tau leaves the velocity unchanged (around 1 µm/s) but strongly reduces the run length and reversal frequency. This holds for both kinesin and dynein, but the inhibition of kinesin is more severe so that dynein-driven movements become dominant. Because the affinity of MAPs to microtubules is regulated by phosphorylation these observations suggest that vesicle movement should be regulatable by kinases causing the detachment of MAPs from microtubules.

Indeed, when MARK2 is induced by addition of doxycyclin in CHO cells there is a dramatic effect on vesicle behavior (Fig. 4). The predominant MAP in CHO cells is a variant of MAP4, one of the high-molecular weight MAPs that control microtubule dynamics (Bulinski and Borisy, 1980; Olson et al., 1995). If the endogenous MAP4 represents obstacles to vesicles on the microtubule track the detachment of MAP4 should facilitate movement. This is indeed seen in the representative traces of Fig. 4 a. The distances traversed during the observation time are normally small (a few micrometers) because there are many kinks where the vesicles change direction. However, induction of MARK2 leads to much more extended tracks (Fig. 4 b). The instantaneous velocities are not affected by MARK ($\sim$1 µm/s; Fig. 4 c), but the reversal frequencies decrease by $\sim$50% (Fig. 4 d), and the run lengths increase by $\sim$50% in both directions (Fig. 4 e). Because MARK2 phosphorylates MAP4 or other MAPs at KXGS motifs in the repeat domain and de-

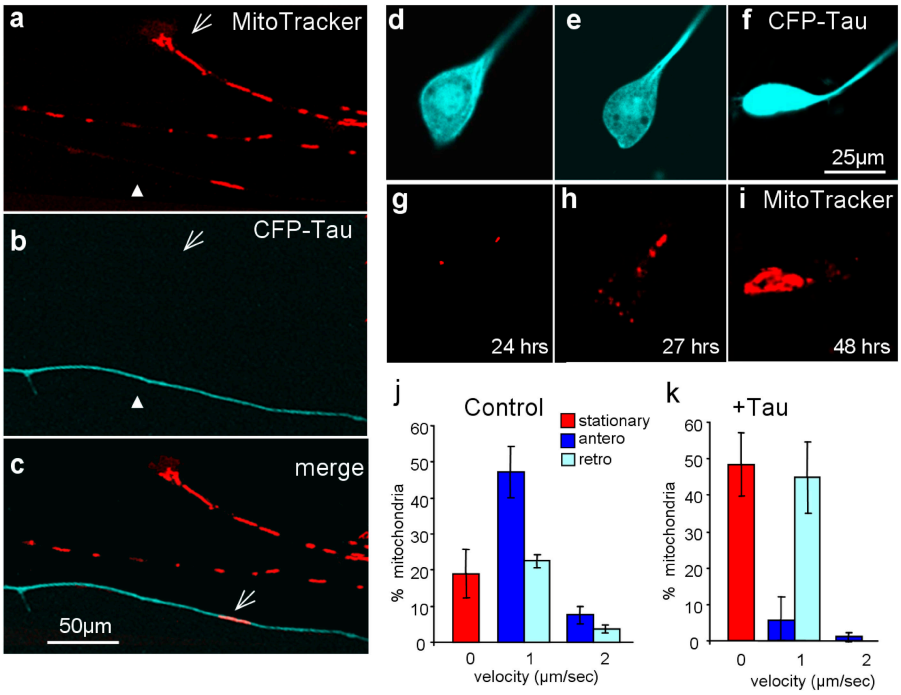

Figure 5. **Distributions of mitochondria in RGC axons, 48 h after transfection with Tau by adenovirus.** (a–c) Field of axons stained with MitoTracker (a), CFP-Tau (b), and merge (c). Mitochondria are frequent in normal axons, but have almost disappeared from tau-transfected axons (see bottom axon in b and c, blue, closed arrowheads). (d–f) Expression of tau with time after transfection, and (g–i) corresponding clustering of mitochondria in cell body. Tau gradually moves out into the axon, whereas mitochondria accumulate in the cell body. (j and k) Quantification of mitochondria movements in controls (j) and tau-transfected cells (k). In control cells, anterograde movements dominate (55%, dark blue bar), in tau-transfected cells anterograde transport decreases (to 7%), immobile particles increase (to 50%, red bar), and retrogradely moving particles increase (to 45%, light blue bar). Error bars indicate SEM.

taches them from microtubules (Illenberger et al., 1996), these results argue that vesicle movement is facilitated and can indeed be regulated locally on the microtubule surface by MAP phosphorylation. This effect is opposite to the transport inhibition by elevated MAP expression (demonstrated in Fig. 1 by the clustering of mitochondria), so that MAPs and their kinases can be regarded as antagonistic with respect to microtubule-based vesicle trafficking.

To check whether the movements of other types of vesicles or organelles were similarly affected by inducing MARK2 and subsequent phosphorylation of MAPs, we studied lysosomes and mitochondria labeled with fluorescent dyes. Generally, organelles differ from vesicles in that they spend only a small fraction of their time (<10%) undergoing directed movement, whereas the majority of time is spent with no motion or only Brownian motion (local fluctuations <0.3 μm/s; Trinczek et al., 1999). Fig. 4 f shows an overlay of lysosomes during an observation time of 60 s. Linear tracks of dots represent directed motion, clusters of dots show Brownian motion, and single dots correspond to particles sitting still. When analyzing moving particles (Fig. 4 g), we find that the instantaneous velocity is independent of whether MARK is induced or not (~0.8 μm/s), but the run length rises conspicuously (approximately twofold). A similar behavior is found for mitochondria (unpublished data). This means that organelles respond to MARK induction similarly to exocytotic vesicles by increasing the run length but not the local velocity. We further investigated endocytotic vesicles labeled with GFP-β2-adaptin, one of the cofactors of the AP-2 adaptin complex of clathrin-coated vesicles (Laporte et al., 1999). Because of their high mobility these vesicles generated a strong background throughout the cytoplasm, and they frequently left the plane of focus which made tracking difficult (Fig. 4 h). In the analysis (Fig. 4 i) we, therefore, included only particles moving within the focal plane, with defined start and stop points. Nevertheless, the same picture emerged: MARK induction had almost no effect on the instantaneous velocity (~1.1 μm/s) but increased the run length by almost twofold (from 3 to 5 μm).

Effect of MARK on axonal transport

The results described thus far were derived from CHO cells because these cells are readily transfected, the microtubule network can be observed, and the proteins are accessible to biochemical analysis. However, for observing effects of transport inhibition that may matter in neurodegeneration we had to turn to differentiated neurons. After a search for suitable cell types we focused on chicken RGCs. Explants of these cells can be obtained from chicken retinae and develop numerous axons in culture with a well-defined polarity which facilitates the measurement of vesicle and organelle movements. The cells can also be transfected with high efficiency (80%) using adenoviral vectors, enabling one to observe the effects of tau (tagged with CFP), MARK2 (tagged with YFP or CFP), and organelles visualized by live stains. In the following description we focus on two examples, mitochondria (stained with MitoTracker red) and vesicles carrying APP, because APP, like tau, plays a crucial role in AD. They are clearly visualized by confocal microscopy and the influence of tau or MARK2 are easily quantified.

One aim of the experiments is to demonstrate the correlation between MARK activity, tau phosphorylation, and organelle movements in the same cell. In the RGC axons of Fig. 5 mitochondria show a roughly uniform distribution with a density around 0.17 particles/μm (Fig. 5 a). Most of these (55%) move anterogradely while the growth cone is advancing; smaller fractions move retrogradely (~26%) or are stationary during the period of observation (24 min; Fig. 5 j). When these cells are transfected with CFP-tau the characteristics of movement change dramatically: over the time of 24 h, most mito-

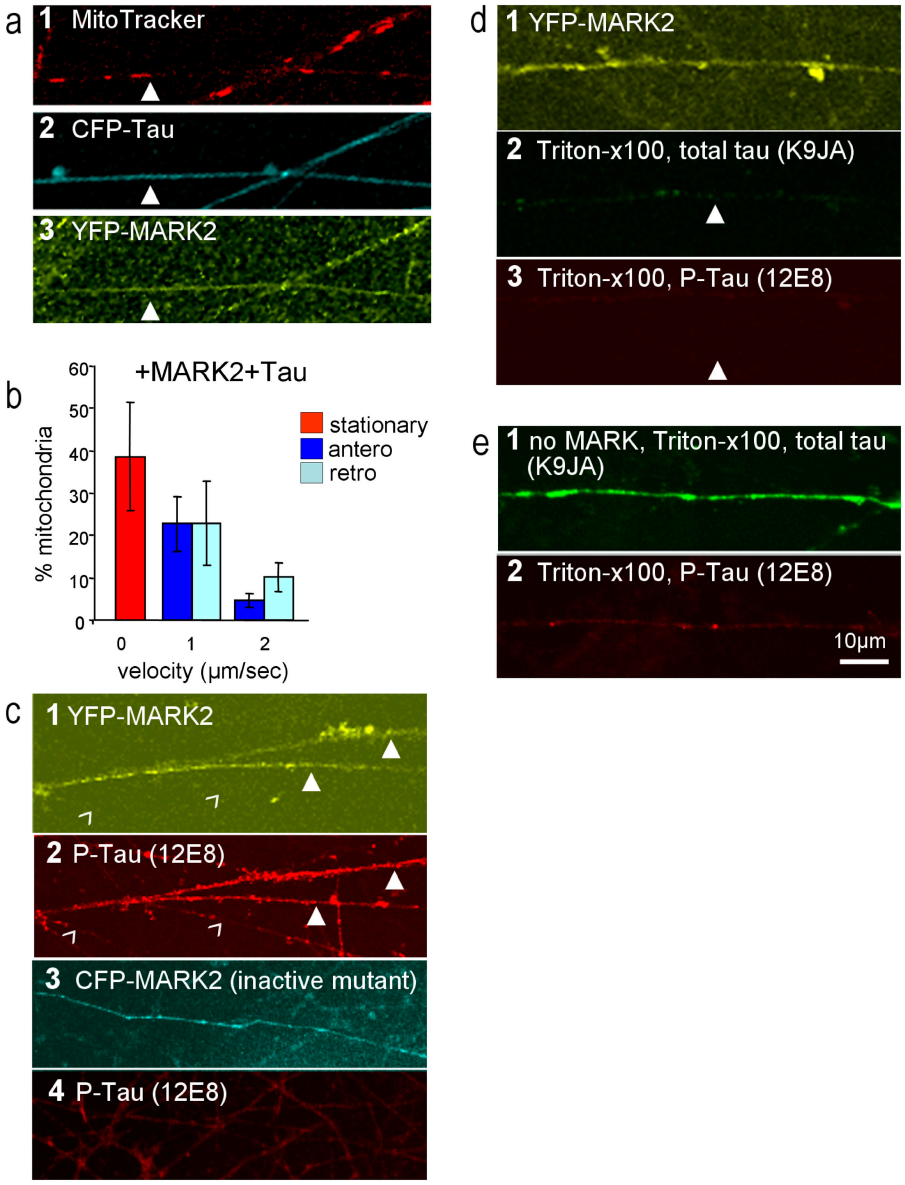

Figure 6. **Recovery of anterograde movements of mitochondria by coexpression of tau and MARK2.** (a,1–3) Axons of RGCs stained for mitochondria (MitoTracker, a 1), CFP-tau (a 2), YFP-MARK2 (a 3). Numerous mitochondria are present in axons, in spite of the presence of tau, because the phosphorylation of tau by MARK detaches it from microtubules and facilitates transport (closed arrowheads). (b) Velocity histogram of mitochondria. Note the substantial recovery of anterograde transport (dark blue bars) after coexpression with MARK2 (compare with Fig. 5 k, transfection of tau only). Error bars indicate SEM. (c, 1–4) Axons showing YFP-MARK2 (c 1) and phospho-Tau (at KXGS motifs, antibody 12E8, c 2, closed arrowheads). Axons after transfection with inactive CFP-MARK2 (c 3), which fails to increase the phosphorylation of KXGS motifs of tau (c 4, antibody 12E8 shows only background staining). (d, 1–3) Axons after transfection of cells with YFP-MARK2 (d 1) and then extracted with Triton X-100 and stained for total Tau (antibody K9JA, d 2) phospho-Tau (antibody 12E8, d 3). Note that Tau phosphorylated at KXGS motifs disappears because it is not attached to microtubules (closed arrowheads). (e, 1 and 2) Axons not transfected with MARK, extracted with Triton X-100, show strong staining with Tau (K9JA, e 1) but not with phospho-Tau (12E8, e 2).

chondria leave the axon and accumulate in the cell body because the dynein-mediated retrograde traffic dominates (Fig. 5, d–i). The density of mitochondria in the axons decreases strongly (0.08 particles/µm after 24 h; Fig. 5 c, arrow), the fraction of anterograde movements drops below 10%, and stationary or retrograde particles increase to nearly 50% (Fig. 5 k). This feature corresponds to the clustering of mitochondria in the cell body around the MTOC for CHO or N2a cells (Fig. 1, b, d, and f), and analogous observations apply to other cell organelles (e.g., lysosomes, peroxisomes) or transport vesicles (e.g., APP-containing vesicles; Stamer et al., 2002). Note that in spite of the retrograde flow of mitochondria, the expressed tau can move forward and fills the axon homogeneously, illustrating that the transport of tau (which is part of slow axonal transport; Mercken et al., 1995) differs from the fast axonal transport of vesicles and organelles.

The next question was whether the inhibitory effect of tau could be relieved by removing tau from microtubules. We transfected RGCs with CFP-tau and YFP-MARK2, both proteins were expressed and became distributed along the axons (Fig. 6 a, 1–3). This has striking consequences for mitochondrial movements (Fig. 6 b): anterograde movements became substantially reactivated (~30%); the fraction of stationary particles decreased (compare Fig. 6 b with Fig. 5 k); and the density of particles increased again. A strong reaction of the 12E8 antibody appeared, revealing that tau was phosphorylated at the KXGS motifs (Fig. 6 c, 2). The phosphorylation of tau was accompanied by its removal from microtubules: if cells transfected with tau and MARK2 (Fig. 6 d, 1) were extracted with Triton X-100 the reaction with antibody 12E8 was lost (Fig. 6 d, 3), indicating that the phosphorylated tau was indeed detached from microtubules, and only traces of unphosphorylated tau remained in the axon (Fig. 6 d, 2). This is in strong contrast to cells not transfected with MARK where extraction by Triton X-100 does not remove tau from microtubules (Fig. 6 e, 1) and tau remains unphosphorylated at KXGS motifs (Fig. 6 e, 2). We conclude that the blockade of traffic was relieved after removing tau from the tracks by phosphorylation at the

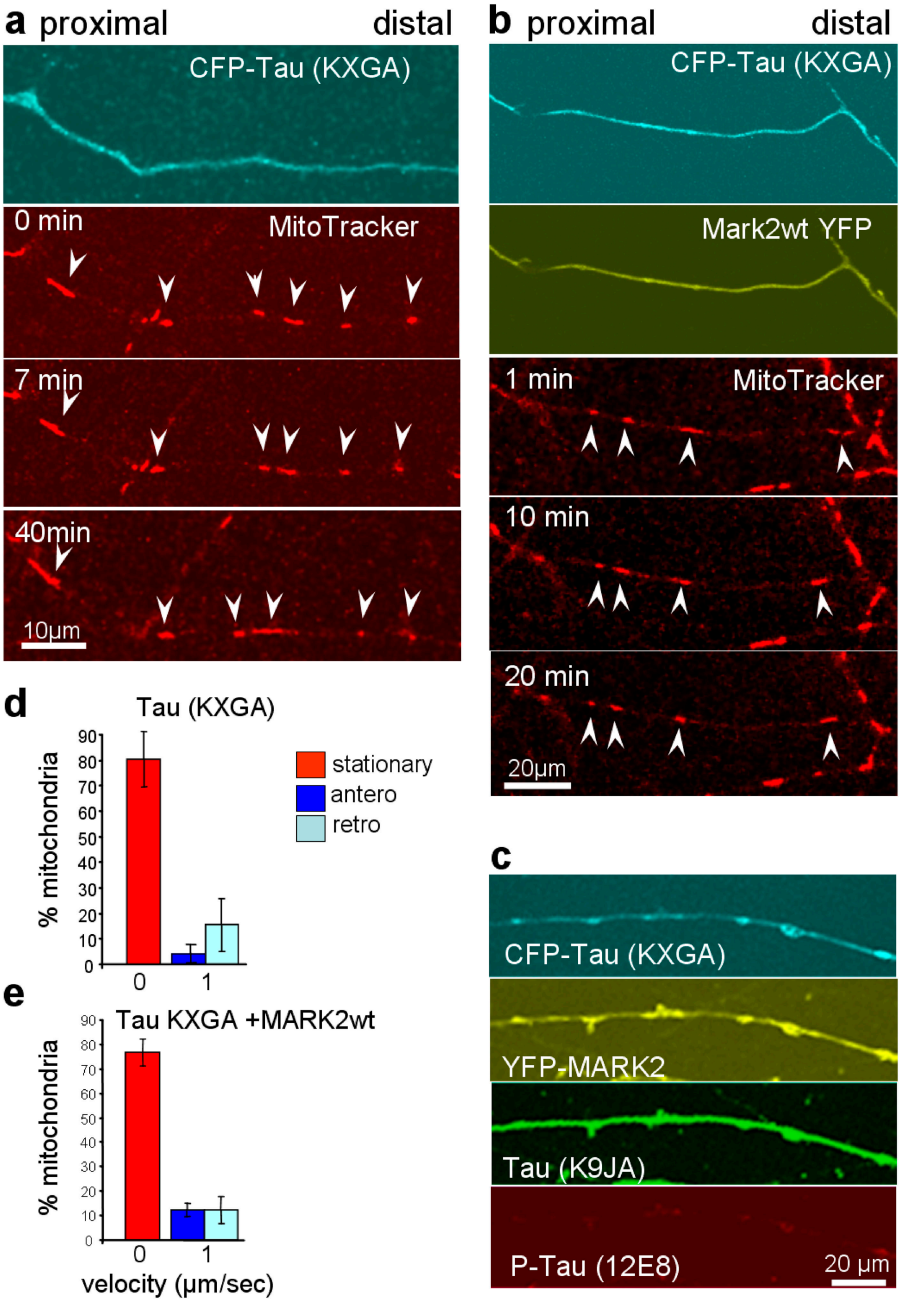

Figure 7. **Non-phosphorylatable tau blocks traffic and cannot be relieved by MARK2.** (a) RGC axon transfected with CFP-tau/KXGA lacking phosphorylation sites by MARK (top, blue). Most mitochondria are immobile (compare arrowheads in middle and bottom panels). (b) Axons transfected with CFP-tau/KXGA and YFP-MARK2 (first and second panel). Mitochondria are still immobile, despite the presence of MARK2 (panels 3 and 4). (c) Axon transfected with CFP-tau/KXGA (top, blue) and YFP-MARK2 (middle, yellow), stained with antibody 12E8 (bottom, red). Note that 12E8 reaction has disappeared because the KXGS motifs are absent. (d) Histogram of mitochondria mobility in tau/KXGA transfected cells (see panel a, showing that ~80% are immobile, only a minority moves antero- or retrogradely. (e) Histogram of mitochondria mobility in tau/KXGA and MARK2 transfected cells, showing that MARK2 does not rescue mobility when tau cannot be phosphorylated. Error bars indicate SEM.

KXGS motifs. Thus, MARK counteracts the inhibitory effect of tau. This interpretation was checked by several controls. Transfection of RGCs with GFP had only a minor effect, most mitochondria moved anterogradely (~50%), only a small fraction were in the pause state (~30%), underscoring that GFP is a neutral marker (unpublished data). The same was true for the kinase-dead mutant of MARK2 (Fig. 6 c, 3), indicating that the effect of MARK was due to its kinase activity. Like active MARK2 or GFP, the inactive mutant was also distributed evenly along the axon (Fig. 6 c, 3), and there was no phosphorylation of tau in the repeat domain above background (judging by 12E8 immunofluorescence; Fig. 6 c, 4). Finally, we constructed an adenovirus vector encoding a mutant CFP-tau where all four KXGS motifs were changed into KXGA so that the targets of MARK2 were eliminated. Transfection in RGCs caused a strong inhibition of transport, similar to wild-type tau (compare Fig. 7, a and d with Fig. 5, j and k). However, in this case the cotransfection with MARK2 was not able to induce phosphorylation of tau or to rescue the mobility of mitochondria (compare Fig. 7, b, c, and e with Fig. 6 b), showing that blockage of traffic by tau and rescue by MARK2 requires phosphorylatable KXGS motifs on tau.

Similar results on traffic inhibition were obtained with APP-vesicles (labeled with YFP) as a function of tau and MARK. In control RGCs, the majority of APP vesicles (80%) moved rapidly anterogradely with velocities up to 7 µm/s, a small fraction (~20%) moved retrogradely, and only very few were in a pause state during the period of observation (20 min; Fig. 8). Expression of tau reversed the net flow of APP vesicles so that very few particles remained in the axons after 24 h (only

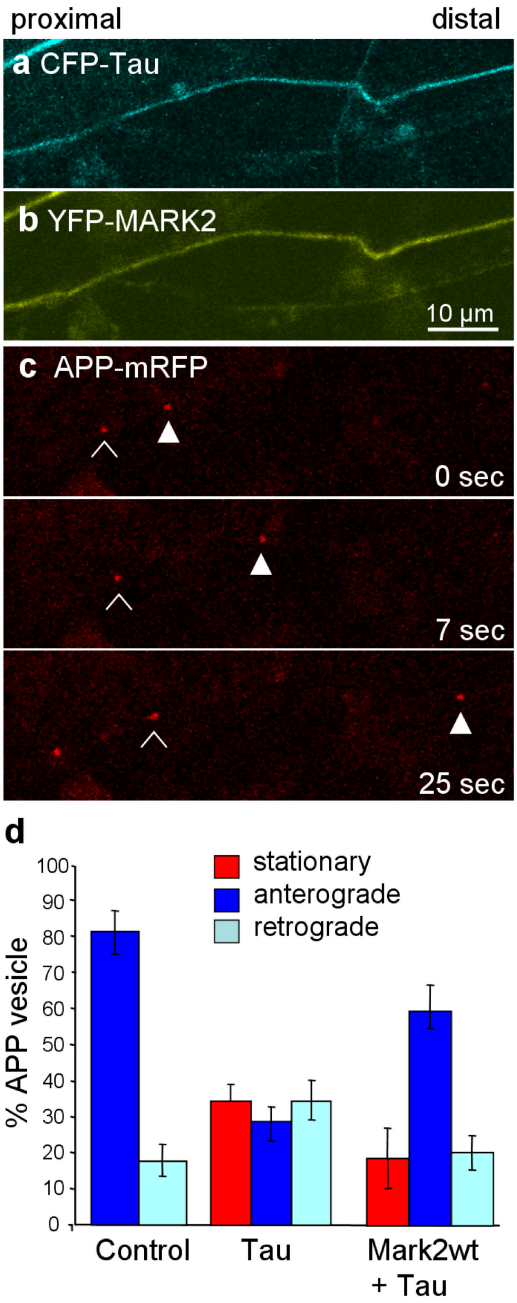

Figure 8. **Recovery of anterograde transport of APP vesicles after coexpression of tau and MARK2.** (a–c) RGC axon transfected with CFP-tau (a), YFP-MARK2 (b), and APP-mRFP (c). The time series in panel c shows recovery of anterograde movements. Open and closed arrowheads show two vesicles moving to the right at different speeds. (d) Histogram showing APP vesicle movements in control (left), after tau transfection (middle), after cotransfection of tau and MARK2 (right). In control cells almost all vesicles are mobile, and anterograde movements dominate. After tau transfection ~40% of vesicles become immobile, and the net flow becomes retrograde. MARK2 partially relieves the inhibition by tau, the net flow becomes anterograde again.

~30% anterograde movements). However, coexpression of tau and MARK2 lead to a partial rescue of the traffic inhibition, the number of vesicles in the axons increased and the net flow became anterograde again (~60% of particles). This reversal was not seen with the kinase-dead MARK2 mutant or with the KXGA-tau mutant.

Discussion

The path of vesicles and organelles through the cytoplasm depends on multiple factors, tracks, motors, adaptors, address codes, and random fluctuations. For most particles, and particularly for long-haul traffic, microtubules are the predominant tracks, mediated by microtubule motors such as kinesin or dynein and their corresponding adaptors (Lippincott-Schwartz, 1998; Baas, 2002). In nonneuronal cells with a radial microtubule network transport events are often highly irregular: the lengths of coherent runs may be limited by obstacles and Brownian fluctuations, und particles may contain several types of motor protein competing with each other and with different tracks. For cells with compact shapes (e.g., CHO) some lack of fidelity in transport may be tolerable because particles tend to recognize and dock to their destination via receptors and adaptor complexes, irrespective of whether the encounter results from directed or undirected movements. In this scenario, microtubules and their motors impose a directional bias but are not unique determinants. However, directed transport becomes important with asymmetric cells such as neurons where diffusion alone would not suffice to deliver particles to the nerve endings.

How can a cell regulate the directional bias? In the first instance this is achieved by the architecture of the polar tracks and the choice of motors and adaptors. Many studies have shown that directed transport can be upset by interfering with microtubule stability or orientation (Morris and Hollenbeck, 1995). Likewise, inactivation or detachment of motors from their tracks or cargoes leads to loss of motion or predominance of other motors (Tanaka et al., 1998; Rahman et al., 1999; Morfini et al., 2002). A further level of traffic control is the quality of the track surface and the MAPs attached to it. Particle motility can be influenced by different types of MAPs (Sato-Harada et al., 1996; Bulinski et al., 1997; Ebneth et al., 1998; Stamer et al., 2002). This effect tends to be inhibitory because the MAPs occlude the binding sites for motors on microtubules, as seen more directly by single-molecule assays (Seitz et al., 2002). The inhibition leads to an overall bias of particle flow toward the cell interior (Fig. 1).

What are the implications of the control chain linking MARK with tau, microtubules, and motors? Because microtubules and tau are present in neuronal cell bodies and axons, the same distribution would be expected for MARK and its activating kinase, which is indeed observed (Timm et al., 2003). After phosphorylation, the detached tau could float in the cytosol (as seen by the diffuse fluorescence of CFP-tau), but in addition the phospho-tau partly attaches to the actin cytoskeleton (Biernat et al., 2002). A similar phenomenon has been reported for phosphorylated MAP2c in dendrites (Ozer and Halpain, 2000). A further point concerns the interference between motors and tau on the microtubule surface. We previously reported that bound tau reduces the average run length of vesicles in cells (Trinczek et al., 1999), and here we show that MARK increases the run length again. This would imply that MARK clears MAPs off the microtubule tracks, either throughout the cell, or at least locally, for example if MARK were bound to the cargo to be transported. In that case the MAPs could mostly remain associated with microtubules, and only a small fraction would

need to be lifted locally from the microtubule surface. In addition we know from experiments on single motor molecules that in vitro tau does not decrease the run length of kinesin as such but the attachment frequency (Seitz et al., 2002). This apparent discrepancy with the observations in cells can be explained by assuming that a cargo particle contains several motors which operate additively or even in concert (Vale, 2003). Thus if one motor slips off the track, another could take over; but if the attachment rate is lowered by a MAP the coordination is perturbed, resulting in a shorter run length.

In RGC axons the relationship between MARK, tau, and traffic is more easily observable than in CHO cells because the microtubule polarity is unambiguous, and traffic events can be traced over longer distances and time periods. The main five results for the case of mitochondria are as follows. (1) Normal state: the majority of mitochondria move anterogradely, small fractions move retrogradely or pause, and the density of mitochondria is relatively high (Fig. 5, a and j). (2) After tau transfection the density decreases drastically (because most mitochondria accumulate in the cell body; Fig. 5, a, c, and d–i). The remaining axonal mitochondria are mostly stationary, some move back, and only very few still move anterogradely (Fig. 5 k). The final state is an axon nearly devoid of mitochondria and thus vulnerable to oxidative stress and other insults (Stamer et al., 2002). (3) Additional transfection of the cells with MARK partially relieves the inhibition by tau so that organelles can move more freely again, especially in the forward direction (Fig. 6 b; Fig. 8). (4) The MARK-transfected axons show tau phosphorylated at KXGS sites and extractable by Triton X-100, indicating that tau is detached from microtubules (Biernat et al., 2002; Fig. 6 c, 2 and d, 2 and 3). (5) Mutant tau with unphosphorylatable KXGA motifs induces strong transport inhibition, which cannot be rescued by MARK2 (Fig. 7).

MAPs are often considered as static elements stabilizing microtubules, with additional functions such as cross-linking, spacing, or anchoring of other cell constituents. The dynamic behavior of MAPs is usually considered only within the framework of microtubule growth or shrinkage. In cells, MAPs are predominantly bound to microtubules, supporting the notion of structural elements (Cassimeris and Spittle, 2001). Nevertheless, the redistribution of MAPs among microtubules is remarkably dynamic even when there is no change in overall microtubule polymerization, suggesting that there is a rapid on/off equilibration (Olmsted et al., 1989; Bulinski et al., 2001). The major regulation of MAP-microtubule binding is achieved by phosphorylation. Many protein kinases and phosphorylation sites have been described for MAPs, most of which tend to lower their affinity to microtubules. Phosphorylation of MAPs is enhanced in fetal tissue (when microtubules are more dynamic), in mitosis (when microtubules have to rearrange), during neuronal differentiation, and in pathological conditions such as neurodegeneration in Alzheimer's disease (where tau loses the ability to bind and stabilize microtubules due to hyperphosphorylation; Lee et al., 2001). These observations have focused attention on the role of MAP phosphorylation in modulating microtubule stability. However, because MAPs also occupy space on the tracks of motor proteins it seemed possible that the phosphorylation of MAPs had other functions as well. MAPs, in particular tau, can be phosphorylated by many kinases, and most target sites become highly phosphorylated in Alzheimer's disease and related tauopathies. However, the effects of tau phosphorylation at different sites can be quite variable. The target sites of proline-directed kinases (SP or TP motifs) tend to have weak or moderate effects, whereas the KXGS motifs in the repeat domain have a pronounced ability to detach tau from microtubules. Tau's ability to interfere with transport requires microtubule binding (Seitz et al., 2002). Therefore, it appeared that MARK would be a good candidate for reversing the transport inhibition.

There are four kinases of the MARK family in humans (Manning et al., 2002). They phosphorylate the KXGS motifs in the MAP2/MAP4/tau family in a similar fashion (Drewes et al., 1997). MARK and its homologues (e.g., PAR-1 in *C. elegans* and *Drosophila*) are important in establishing asymmetric cell shapes and distributions (Kemphues, 2000; Riechmann and Ephrussi, 2001; Cohen et al., 2004), including NGF-induced neurite outgrowth from neurons (Biernat et al., 2002). The effects of MARK would therefore be visible in various cell types. MARK is itself regulated by phosphorylation of the activation loop by the activating kinase MARKK (Timm et al., 2003). It is thus embedded in a kinase cascade, reminiscent of other cascades that are regulated by intra- or extracellular signals (Cobb and Goldsmith, 2000). Other modes of regulation could be through scaffold proteins such as 14-3-3 (Benton et al., 2002). The triggers of MARK signaling are not well understood, but they appear to include neuronal differentiation signals and oxidative stress (Jenkins and Johnson, 2000; Biernat et al., 2002).

The results summarized in Fig. 9 show that the cell is capable of enhancing the motility of vesicles and organelles by activating the kinase MARK2. This kinase mainly targets the KXGS motifs in MAP4, MAP2, and tau, thereby removing them from the microtubule surface. Conversely, overexpression of MAPs overwhelms the kinase and leads to clogging of tracks and traffic inhibition, independently of the stabilization of microtubules. It is possible that this kinase also explains the phosphorylation-induced enhancement of vesicle motility observed by other authors (Lopez and Sheetz, 1995; Sato-Harada et al., 1996). The mechanism appears to be similar with all cargoes and MAPs studied so far (demonstrated here for the case of VSV-G vesicles, clathrin-coated vesicles, APP-vesicles, lysosomes, and mitochondria; Figs. 4, 6, and 8). It is based on an apparent extension of the run length without change in the instantaneous velocities. This means that the motor activity itself is not affected, but the probability of motor attachment is increased because there are fewer MAPs as obstacles in their way.

MARK was originally identified by a search for the kinase that phosphorylates tau at sites that appear at early stages of Alzheimer's neurodegeneration and that are critical for tau's binding and stabilization (Augustinack et al., 2002). In Alzheimer's disease, two proteins are mainly responsible for the abnormal aggregates, tau and the Aβ peptide, whose relationship is still a matter of debate. The observation that tau inhibits axonal traffic, including that of APP, may shed new light on the relationship. If APP remains in the cell body for extended periods because anterograde traffic is blocked by tau there is a

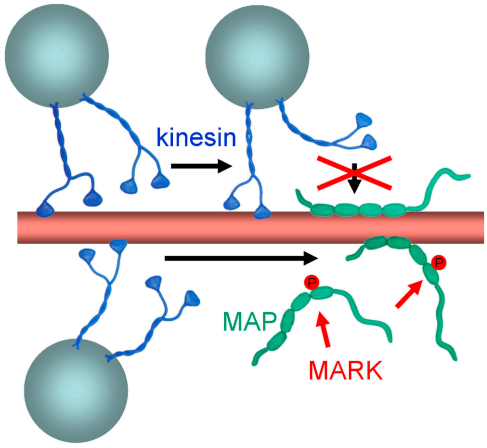

Figure 9. **Model of MAPs and MARK regulating the movement of motors along microtubules.** (Top) Unphosphorylated MAPs are attached to microtubules and present obstacles to motors such as kinesin (short run length, inhibition of attachment of motors). (Bottom) MAPs phosphorylated by MARK detach from microtubules and thus clear the path for motors.

higher probability of intracellular cleavage of APP and generation of Aβ peptides which are toxic for the neuron. We speculate that the cell responds to this challenge by activating the kinase MARK which would free up the intracellular pathways and thereby reduce the generation of Aβ. Thus, the early phosphorylation of tau at KXGS motifs observed in Alzheimer's disease could be seen as the cell's defense strategy to keep traffic pathways open and to reduce the generation of toxic byproducts. This mechanism would provide an interesting opportunity for identifying factors that cause the degeneration of neurons, and for designing methods to relieve it. Finally, we note that there is increasing evidence that neurodegeneration is accompanied by defects in transport. This could be due to a defect or an unbalance of motors, adaptors of cargoes, or tracks and their modifiers, as in the case described here (for review see Goldstein, 2003). The mechanisms and responsible proteins may differ, but the common principle is that even slight perturbances of the traffic system has severe consequences for neurons whose survival depends on active transport.

Materials and methods

Plasmids, cell culture, transfection, and fluorescent labeling
cDNAs encoding MAP2c, MAP4-BD, and MARK2 were inserted into a derivative of pRc/CMV (Invitrogen) using synthetic linkers, which introduced an NH_2-terminal HA-epitope tag, to yield pEUHAMAP2c, pEUHATagMAP4-BD (provided by J. Olmsted, University of Rochester, Rochester, NY; Ebneth et al., 1999) and pEUHATagMARK2 (Drewes et al., 1997). For doxycyclin-inducible expression, epitope-tagged MARK2 was cloned into pUHD10-3 to yield pINDMARK2 (Drewes et al., 1997). pUHD10-3 were provided by H. Bujard (ZMBH, Heidelberg, Germany). Stably transfected MARK2-inducible CHO cells (CHO-I3) were cloned as described previously (Drewes et al., 1997). Induction of MARK2 was achieved by addition of 1 μg/ml doxycyclin (Sigma-Aldrich) into the medium and incubation for 12–18 h. Induction of HA-tagged MARK2 in cells prepared for motion analysis was checked by immunofluorescence. Cells seeded on coverslips were fixed with 2% (wt/vol) PFA. Primary antibody incubation was performed in PBS, 3% goat serum for 1 h at 37°C (polyclonal rabbit HA tag antibody; MoBiTec; tubulin antibody DM1A; Sigma-Aldrich). Fluorescently labeled secondary antibodies were applied at 1:200 dilution for 1 h at 37°C (Dianova). Cells were then sealed with permafluor (Dianova) and analyzed under an Axioplan microscope (Carl Zeiss MicroImaging, Inc.) equipped with an 100× oil immersion objective (Carl Zeiss MicroImaging, Inc.) using standard FITC and TRITC filters. Cells were grown in Ham's F12 medium with 10% FCS and 2 mM glutamine (Biochrom) at 37°C and 5% CO_2 in a humidified chamber. For transient transfection of the CHO-I3 cells with GFP-VSVG plasmid (provided by S. Scales and T. Kreis, University of Geneva, Geneva, Switzerland; Scales et al., 1997) and with GFP-β2-adaptin plasmid (provided by S. Laporte and M. Caron, Duke University, Durham, NC; Laporte et al., 1999), cells were seeded at 70% confluency onto LabTek chambered cover glass (Nunc) and transfected with 1 μg of plasmid DNA in the presence of DOTAP (Boehringer) following the manufacturer's instructions. Lysosomes and mitochondria were fluorescently labeled by 1 μM LysoTracker or 200 nM MitoTracker red (Molecular Probes) for 15 min.

For fluorescent staining of the AP-2/clathrin-coated vesicles, cells were transfected overnight with 1 μg of the EGFP/β2-adaptin vector (β2-adaptin gene cloned into the SmaI–BamHI site of pEGFP-C1 (CLONTECH Laboratories, Inc.) using DOTAP (Boehringer). Before data acquisition the chamber was sealed with baysilone (Bayer) to keep the pH of the culture medium constant at pH 7.2–7.4. Temperature was held constant at 35°C by an air stream. Samples were observed with an Axiovert 10 (Carl Zeiss MicroImaging, Inc.) equipped with a 63×/1.4 NA oil-immersion objective and standard fluorescein filters.

Stable transfection of CHO cells
Stably tau transfected CHO cells were generated as described previously (Ebneth et al., 1998). For expressing MAP2c or MAP4-BD in CHO cells, ~60% confluent CHO cells were transfected with 2 μg of plasmid DNA pEUHATagMAP4-BD or pEUHAMAP2c encoding MAP4-BD or MAP2c, and Lipofectamine following the manufacturer's protocol (Invitrogen Life Technologies). Stably transfected cells were selected by growing them in 800 μg/ml geneticin (G-418). After incubation for additional 2–3 wk, cells were cloned by limiting dilution and screened for MAP4-BD–or MAP2c-expressing cells by immunofluorescence and PCR.

Adenovirus vectors encoding fluorescent fusion proteins
Recombinant adenoviruses (CFP-htau40, nonphosphorylatable CFP-htau40/KXGA, APP-YFP, APP-mRFP, YFP-MARK2 wild-type, or dominant negative mutant CFP-MARK2/T208A/S212A) were generated following He et al. (1998) (see Online supplemental material).

Live cell light microscopy
RGCs were prepared as described previously (Stamer et al., 2002; see Online supplemental material). For visualizing the transfection of RGCs and the movement of vesicles and organelles the cells were observed on a confocal microscope (model LSM510; Carl Zeiss MicroImaging, Inc.), kept at 37°C by air heating and supplied with 5% CO_2. Images were taken every 4 s for tracking of vesicles and every 8 s for mitochondria, using a 63× objective, beam path, and laser settings for YFP, CFP, or rhodamine fluorescence. Error bars in histograms indicate SEM throughout.

Antibodies and dyes
Rat monoclonal anti-tubulin antibody YL1/2 and mouse mAb DM1A were purchased from Serotec and Sigma-Aldrich, and used at 1:2,000. Polyclonal rabbit anti tau-antibody K9JA was purchased from DakoCytomation, mAb 12E8 against tau (phosphorylated KXGS motifs in the repeat domain, Ser 262 and 356) was a gift from P. Seubert (Elan Pharma, South San Francisco, CA), antibodies against peroxisomes were from W. Just (University of Heidelberg, Heidelberg, Germany). The clone of mRFP was provided by R. Tsien (University of California, San Diego, La Jolla, CA). All fluorescent (TRITC, FITC, and AMCA) secondary antibodies were purchased from Dianova.

Immunofluorescence
Cells were fixed in methanol or 4% PFA and incubated with antibodies. Cells were examined with an Axioplan fluorescence microscope (Carl Zeiss MicroImaging, Inc.) equipped with an 100× oil-immersion objective and filters optimized for triple-label experiments (FITC-, TRITC-, and AMCA-fluorescence) or with an LSM510 confocal microscope using a 63× objective. Changes in mitochondrial distribution were quantified by measuring the cell area occupied by mitochondria, compared with the whole cell, after subtracting the area occupied by the nucleus.

Online supplemental material
Online supplemental material describes the generation of adenoviruses and the transfection of retinal ganglion neurons. This is available at http://www.jcb.org/cgi/content/full/jcb.200401085/DC1.

We are grateful to K. Neumann and N. Habbe for excellent technical assistance, Dr. S. Kundu for experiments on MAP4-transfected cells, Dr. R. Vogel for help with adenoviral vectors for transfection, and A. Marx for help with data analysis. We thank Dr. W. Just for antibodies against peroxisomes, Dr. S. Laporte and Dr. M. Caron for the plasmid of β2-GFP-adaptin, Dr. P. Seubert for 12E8 antibody, Dr. R. Tsien for mRFP, and Dr. A. Marx for help with data analysis.

The project was supported in part by a grant from the Deutsche Forschungsgemeinschaft.

Submitted: 16 January 2004
Accepted: 30 August 2004

References

Augustinack, J.C., A. Schneider, E.-M. Mandelkow, and B. Hyman. 2002. Specific tau phosphorylation sites correlate with severity of neuronal cytopathology in Alzheimer's disease. *Acta Neuropathol. (Berl.).* 103:26–35.

Baas, P.W. 2002. Microtubule transport in the axon. *Int. Rev. Cytol.* 212:41–62.

Benton, R., I.M. Palacios, and D. St. Johnston. 2002. *Drosophila* 14-3-3/PAR-5 is an essential mediator of PAR-1 function in axis formation. *Dev. Cell.* 3:659–671.

Biernat, J., Y.Z. Wu, T. Timm, Q. Zheng-Fischhofer, E. Mandelkow, L. Meijer, and E.-M. Mandelkow. 2002. Protein kinase MARK/PAR-1 is required for neurite outgrowth and establishment of neuronal polarity. *Mol. Biol. Cell.* 13:4013–4028.

Bulinski, J.C., and G.G. Borisy. 1980. Widespread distribution of a 210,000 mol wt microtubule-associated protein in cells and tissues of primates. *J. Cell Biol.* 87:802–808.

Bulinski, J.C., T.E. McGraw, D. Gruber, H.L. Nguyen, and M.P. Sheetz. 1997. Overexpression of MAP4 inhibits organelle motility and trafficking in vivo. *J. Cell Sci.* 110:3055–3064.

Bulinski, J.C., D.J. Odde, B.J. Howell, T.D. Salmon, and C. Waterman-Storer. 2001. Rapid dynamics of the microtubule binding of ensconsin in vivo. *J. Cell Sci.* 114:3885–3897.

Cassimeris, L., and C. Spittle. 2001. Regulation of microtubule-associated proteins. *Int. Rev. Cytol.* 210:163–226.

Cobb, M., and E. Goldsmith. 2000. Dimerization in MAP kinase signalling. *Trends Biochem. Sci.* 25:7–9.

Cohen, D., P. Brennwald, E. Rodriguez-Boulan, and A. Müsch. 2004. Mammalian PAR-1 determines epithelial lumen polarity by organizing the microtubule cytoskeleton. *J. Cell Biol.* 164:717–727.

Drewes, G., A. Ebneth, U. Preuss, E.-M. Mandelkow, and E. Mandelkow. 1997. MARK—a novel family of protein kinases that phosphorylate microtubule-associated proteins and trigger microtubule disruption. *Cell.* 89:297–308.

Drubin, D., and M. Kirschner. 1986. Tau protein function in living cells. *J. Cell Biol.* 103:2739–2746.

Ebneth, A., R. Godemann, K. Stamer, S. Illenberger, B. Trinczek, E.-M. Mandelkow, and E. Mandelkow. 1998. Overexpression of tau protein alters kinesin-dependent trafficking of vesicles, mitochondria, and endoplasmic reticulum: implications for Alzheimer's disease. *J. Cell Biol.* 143:777–794.

Ebneth, A., G. Drewes, E.-M. Mandelkow, and E. Mandelkow. 1999. Phosphorylation of MAP2c and MAP4 by MARK kinases leads to the destabilization of microtubules in cells. *Cell Motil. Cytoskeleton.* 44:209–224.

Garcia, M.L., and D.W. Cleveland. 2001. Going new places using an old MAP: tau, microtubules and human neurodegenerative disease. *Curr. Opin. Cell Biol.* 13:41–48.

Goldstein, L.S. 2003. Do disorders of movement cause movement disorders and dementia? *Neuron.* 40:415–425.

Gossen, M., and H. Bujard. 2002. Studying gene function in eukaryotes by conditional gene inactivation. *Annu. Rev. Genet.* 36:153–173.

Hagiwara, H., H. Yorifuji, R. Sato-Yoshitake, and N. Hirokawa. 1994. Competition between motor molecules kinesin and cytoplasmic dynein., and fibrous microtubule-associated proteins in binding to microtubules. *J. Biol. Chem.* 269:3581–3589.

He, T.C., S. Zhou, L.T. da Costa, J. Yu, K.W. Kinzler, and B. Vogelstein. 1998. A simplified system for generating recombinant adenoviruses. *Proc. Natl. Acad. Sci. USA.* 95:2509–2514.

Illenberger, S., G. Drewes, B. Trinczek, J. Biernat, H.E. Meyer, J.B. Olmsted, and E.-M. Mandelkow. 1996. Phosphorylation of microtubule associated proteins MAP2 and MAP4 by the protein kinase p110/mark: phosphorylation sites and regulation of microtubule dynamics. *J. Biol. Chem.* 271:10834–10843.

Jenkins, S.M., and G.V. Johnson. 2000. Microtubule/MAP affinity regulating kinase MARK is activated by phenylarsine oxide in situ and phosphorylates tau within its microtubule-binding domain. *J. Neurochem.* 74:1463–1468.

Kamal, A., and L.S. Goldstein. 2002. Principles of cargo attachment to cytoplasmic motor proteins. *Curr. Opin. Cell Biol.* 14:63–68.

Kemphues, K. 2000. PARsing embryonic polarity. *Cell.* 101:345–348.

Kosik, K.S., and L. McConlogue. 1994. Microtubule-associated protein function: lessons from expression in spodoptera frugiperda cells. *Cell Motil. Cytoskeleton.* 28:195–198.

Laporte, S.A., R.H. Oakley, J. Zhang, J.A. Holt, S.S. Ferguson, M.G. Caron, and L.S. Barak. 1999. The beta2-adrenergic receptor/beta-arrestin complex recruits the clathrin adaptor AP-2 during endocytosis. *Proc. Natl. Acad. Sci. USA.* 96:3712–3717.

Lee, K.D., and P.J. Hollenbeck. 1995. Phosphorylation of kinesin in vivo correlates with organelle association and neurite outgrowth. *J. Biol. Chem.* 270:5600–5605.

Lee, V.M., M. Goedert, and J.Q. Trojanowski. 2001. Neurodegenerative tauopathies. *Annu. Rev. Neurosci.* 24:1121–1159.

Lippincott-Schwartz, J. 1998. Cytoskeletal proteins and Golgi dynamics. *Curr. Opin. Cell Biol.* 10:52–59.

Lopez, L.A., and M.P. Sheetz. 1993. Steric inhibition of cytoplasmic dynein and kinesin motility by MAP2. *Cell Motil. Cytoskeleton.* 24:1–16.

Lopez, L.A., and M.P. Sheetz. 1995. A microtubule-associated protein (MAP2) kinase restores microtubule motility in embryonic brain. *J. Biol. Chem.* 270:12511–12517.

Manning, G., D.B. Whyte, R. Martinez, T. Hunter, and S. Sudarsanam. 2002. The protein kinase complement of the human genome. *Science.* 298:1912–1934.

Mercken, M., I. Fischer, K.S. Kosik, and R.A. Nixon. 1995. Three distinct axonal transport rates for tau, tubulin, and other microtubule-associated proteins: evidence for dynamic interactions of tau with microtubules in vivo. *J. Neurosci.* 15:8259–8267.

Morfini, G., G. Szebenyi, R. Elluru, N. Ratner, and S.T. Brady. 2002. Glycogen synthase kinase 3 phosphorylates kinesin light chains and negatively regulates kinesin-based motility. *EMBO J.* 21:281–293.

Morris, R.L., and P.J. Hollenbeck. 1995. Axonal transport of mitochondria along microtubules and F-actin in living vertebrate neurons. *J. Cell Biol.* 131:1315–1326.

Olmsted, J.B., D. Stemple, W. Saxton, B. Neighbors, and J.R. Mcintosh. 1989. Cell cycle–dependent changes in the dynamics of MAP2 and MAP4 in cultured cells. *J. Cell Biol.* 109:211–223.

Olson, K.R., J.R. McIntosh, and J.B. Olmsted. 1995. Analysis of MAP 4 function in living cells using green fluorescent protein (GFP) chimeras. *J. Cell Biol.* 130:639–650.

Ozer, R., and S. Halpain. 2000. Phosphorylation-dependent localization of microtubule-associated protein MAP2c to the actin cytoskeleton. *Mol. Biol. Cell.* 11:3573–3587.

Rahman, A., A. Kamal, E.A. Roberts, and L.S. Goldstein. 1999. Defective kinesin heavy chain behavior in mouse kinesin light chain mutants. *J. Cell Biol.* 146:1277–1288.

Riechmann, V., and A. Ephrussi. 2001. Axis formation during *Drosophila* oogenesis. *Curr. Opin. Genet. Dev.* 11:374–383.

Sato-Harada, R., S. Okabe, T. Umeyama, Y. Kanai, and N. Hirokawa. 1996. Microtubule-associated proteins regulate microtubule function as the track for intracellular membrane organelle transports. *Cell Struct. Funct.* 21:283–295.

Scales, S.J., R. Pepperkok, and T.E. Kreis. 1997. Visualization of ER-to-Golgi transport in living cells reveals a sequential mode of action for COPII and COPI. *Cell.* 90:1137–1148.

Seitz, A., H. Kojima, K. Oiwa, E.-M. Mandelkow, Y.H. Song, and E. Mandelkow. 2002. Single-molecule investigation of the interference between kinesin, tau and MAP2c. *EMBO J.* 21:4896–4905.

Stamer, K., R. Vogel, E. Thies, E. Mandelkow, and E.-M. Mandelkow. 2002. Tau blocks traffic of organelles, neurofilaments, and APP vesicles in neurons and enhances oxidative stress. *J. Cell Biol.* 156:1051–1063.

Tanaka, Y., Y. Kanai, Y. Okada, S. Nonaka, S. Takeda, A. Harada, and N. Hirokawa. 1998. Targeted disruption of mouse conventional kinesin heavy chain, kif5B, results in abnormal perinuclear clustering of mitochondria. *Cell.* 93:1147–1158.

Terada, S., and N. Hirokawa. 2000. Moving on to the cargo problem of microtubule-dependent motors in neurons. *Curr. Opin. Neurobiol.* 10:566–573.

Timm, T., X.Y. Li, J. Biernat, J. Jiao, E. Mandelkow, J. Vandekerckhove, and E.-M. Mandelkow. 2003. MARKK, a Ste-20-like kinase, activates the polarity-inducing kinase MARK/PAR-1. *EMBO J.* 22:5090–5101.

Trinczek, B., A. Ebneth, E.-M. Mandelkow, and E. Mandelkow. 1999. Tau regulates the attachment/detachment but not the speed of motors in microtubule-dependent transport of single vesicles and organelles. *J. Cell Sci.* 112:2355–2367.

Vale, R.D. 2003. The molecular motor toolbox for intracellular transport. *Cell.* 112:467–480.